Journal for
ImmunoTherapy of Cancer

Antitumor activity of the investigational B7-H3 antibody-drug conjugate, vobramitamab duocarmazine, in preclinical models of neuroblastoma

Chiara Brignole,[1] Enzo Calarco,[1] Veronica Bensa,[1] Elena Giusto,[1] Patrizia Perri,[1] Eleonora Ciampi,[1] Maria Valeria Corrias,[1] Simonetta Astigiano,[2] Michele Cilli,[2] Derik Loo,[3] Ezio Bonvini,[3] Fabio Pastorino [ID],[1] Mirco Ponzoni [ID] [1]

[1]Laboratory of Experimental Therapies in Oncology, IRCCS Istituto Giannina Gaslini, Genova, Italy
[2]Animal Facility, IRCCS Ospedale Policlinico San Martino, Genova, Italy
[3]MacroGenics Inc, Rockville, Maryland, USA

Correspondence to
Dr Fabio Pastorino;
fabiopastorino@gaslini.org

ABSTRACT

Introduction B7-H3 is a potential target for pediatric cancers, including neuroblastoma (NB). Vobramitamab duocarmazine (also referred to as MGC018 and herein referred to as vobra duo) is an investigational duocarmycin-based antibody-drug conjugate (ADC) directed against the B7-H3 antigen. It is composed of an anti-B7-H3 humanized IgG1/kappa monoclonal antibody chemically conjugated through a cleavable valine-citrulline linker to a duocarmycin-hydroxybenzamide azaindole (vc-seco-DUBA). Vobra duo has shown preliminary clinical activity in B7-H3-expressing tumors.

Methods B7-H3 expression was evaluated by flow-cytometry in a panel of human NB cell lines. Cytotoxicity was evaluated in monolayer and in multicellular tumor spheroid (MCTS) models by the water-soluble tetrazolium salt,MTS, proliferation assay and Cell Titer Glo 3D cell viability assay, respectively. Apoptotic cell death was investigated by annexin V staining. Orthotopic, pseudometastatic, and resected mouse NB models were developed to mimic disease conditions related to primary tumor growth, metastases, and circulating tumor cells with minimal residual disease, respectively.

Results All human NB cell lines expressed cell surface B7-H3 in a unimodal fashion. Vobra duo was cytotoxic in a dose-dependent and time-dependent manner against all cell lines (IC50 range 5.1–53.9 ng/mL) and NB MCTS (IC50 range 17.8–364 ng/mL). Vobra duo was inactive against a murine NB cell line (NX-S2) that did not express human B7-H3; however, NX-S2 cells were killed in the presence of vobra duo when co-cultured with human B7-H3-expressing cells, demonstrating bystander activity. In orthotopic and pseudometastatic mouse models, weekly intravenous treatments with 1 mg/kg vobra duo for 3 weeks delayed tumor growth compared with animals treated with an irrelevant (anti-CD20) duocarmycin-ADC. Vobra duo treatment for 4 weeks further increased survival in both orthotopic and resected NB models. Vobra duo compared favorably to TOpotecan-TEMozolomide (TOTEM), the standard-of-care therapy for NB relapsed disease, with tumor relapse delayed or arrested by two or three repeated 4-week vobra duo treatments, respectively. Further increased survival was observed in mice treated with vobra duo in combination with TOTEM. Vobra duo treatment was not associated with body weight loss, hematological toxicity, or clinical chemistry abnormalities.

WHAT IS ALREADY KNOWN ON THIS TOPIC

⇒ Neuroblastoma (NB) remains an incurable and aggressive disease, with limited therapeutic opportunities. NB expresses B7-H3, a molecule that is emerging as a significant target in oncology, owing to its overexpression in many human cancers and minimal expression or absence in normal tissues, its impact on the disease progression, association with poor prognosis, and potential immunosuppressive role.

WHAT THIS STUDY ADDS

⇒ This report explores the potential utility of targeting B7-H3 with vobramitamab duocarmazine (vobra duo) in preclinical models of NB to support its potential utility in the clinical settings. To that effect, in addition to an expanded in vitro activity characterization in several models (including spheroids) complementing the original report on vobra duo (Scribner *et al*, MCT 2020), extensive emphasis has been placed in murine tumor models recapitulating clinical stages of NB together with providing comparison and integration with standard-of-care intervention (TOpotecan-TEMozolomide therapy).

⇒ The duocarmycin payload of vobra duo acts as a DNA alkylator with cytotoxic potential against both proliferating and non-proliferating cells and is a limited substrate for multidrug extrusion mechanisms, factors that differentiate vobra duo from other antibody-drug conjugates. Furthermore, owing to a cleavable linker, vobra duo can exert bystander activity in the tumor microenvironment, addressing the potential escape in case of tumor heterogeneity.

HOW THIS STUDY MIGHT AFFECT RESEARCH, PRACTICE OR POLICY

⇒ We believe the data presented provide a strong rationale for exploring the potential clinical utility of vobra duo in this unmet clinical need.

Conclusion Vobra duo exerts relevant antitumor activity in preclinical B7-H3-expressing NB models and represents a potential candidate for clinical translation.

INTRODUCTION

Originating from neural crest-derived cells undergoing defective sympathetic neuronal differentiation, neuroblastoma (NB) is the most frequent extracranial solid tumor in the pediatric population, accounting for about 7% of all malignancies diagnosed under the age of 15.[1 2] The majority of cases are diagnosed during the first year of life, with a median age at diagnosis of 17 months.[1] Prognosis in NB is heterogeneous, ranging from cases of spontaneous regression to highly metastatic disease at onset, with 50% of patients falling in the latter category.[3 4] The international NB risk group classification reports an overall survival at 5 years of less than 50% for high-risk patients.[5] Such a poor outcome is dictating the urgent search for new therapeutic approaches.

B7-H3 (CD276), a member of the B7 superfamily of transmembrane glycoproteins involved in immune-modulatory functions, is a target of interest in pediatric oncology. Ewing sarcoma, rhabdomyosarcoma, Wilms tumor, multiple central nervous systems tumors, and NB all overexpress B7-H3.[6–10] A specific B7-H3 receptor has not been unequivocally identified and the immunological role of the molecule remains controversial. While some reports support a potential co-stimulatory function, most evidence is consistent with an immunosuppressive role in cancer.[11 12] Accordingly, B7-H3 overexpression in malignancies[13–17] is associated with immune evasion and tumor progression, in addition to drug resistance.[18] Furthermore, B7-H3 protein expression in normal tissues is limited,[19] rendering it particularly attractive as a tumor-associated target antigen.

Antibody-drug conjugates (ADCs), composed of a monoclonal antibody (mAb) conjugated through a chemical linker to a potent cytotoxic drug,[20] combine selective tumor recognition with the high cytolytic activity of small molecules whose systemic administration in free form is typically unfeasible due to their toxicity. ADCs are intended to deliver their payload at tumor sites while sparing healthy tissues, thus limiting off-target toxicity. Following binding to tumor cells, ADCs undergo internalization through receptor-mediated endocytosis with subsequent release of the payload within the lysosomal compartment, followed by cytotoxic cell death. ADCs featuring cleavable linkers release payloads that can diffuse within the tumor microenvironment, promoting the death of neighboring cells through bystander killing. Treatment of tumors with heterogeneous antigen expression can be effectively targeted via this mechanism of action.[21] ADCs have been widely investigated in the last decades for the treatment of hematological and solid malignancies, with several agents currently approved by the Food and Drug Administration (FDA) for clinical use and many more in late phase of clinical development.[22 23]

Vobramitamab duocarmazine (also referred to as MGC018 and herein referred to as vobra duo) is an investigational duocarmycin-based ADC directed against the B7-H3 antigen.[24 25] It is composed of an anti-B7-H3 humanized IgG1/kappa mAb chemically conjugated through a cleavable valine-citrulline linker to a duocarmycin-hydroxybenzamide azaindole (vc-seco-DUBA). Vobra duo has demonstrated preclinical activity against a variety of B7-H3-expressing tumors, including lung, breast, and ovarian cancers when evaluated in vitro and in vivo, as well as in patient-derived xenografts of triple-negative breast, prostate, and head-and-neck cancers.[24]

Vobra duo is currently being evaluated in patients with advanced castration-resistant metastatic prostate cancer, with initial encouraging evidence of antitumor activity.[26] Here, we provide further evidence of vobra duo effectiveness against NB in vitro and in several clinically relevant mouse NB models.

MATERIALS AND METHODS
Cell lines and culture conditions

Human NB cell lines (IMR-32, HTLA-230, SH-SY5Y, SK-N-BE2c, LAN-5, NB-1691),[27–30] murine NB cell lines (Neuro-2a and NX-S2),[31] human Burkitt lymphoma Daudi cell line,[32] were all cultured in high-glucose Dulbecco's Modified Eagle Medium (DMEM) or Roswell Park Memorial Institute-1640 (RPMI-1640) supplemented with 10% of heat-inactivated fetal bovine serum (FBS), 50 IU/mL penicillin G, 50 µg/mL streptomycin sulfate, and 2 mM L-glutamine. Stably luciferase (luc) transduced IMR-32, HTLA-230, LAN-5, SH-SY5Y, SK-N-BE2c, NB-1691 and NX-S2 cell lines (ie, IMR-32-luc, HTLA-230-luc, LAN-5-luc, SH-SY5Y-luc, SK-N-BE2c-luc, NB-1691-luc and NX-S2-luc) were cultured in DMEM, as previously reported.[29] Cell lines were periodically tested for mycoplasma contamination by PCR assay, characterized by cell proliferation and morphology evaluation, and authenticated by multiplex short-tandem repeat profiling (PowerPlex Fusion-24 loci, Promega, Milano, Italy). Multicellular tumor spheroids (MCTS), an in vitro model consisting of scaffold-free, self-assembled spherical cell aggregates, were generated by seeding IMR-32, HTLA-230, LAN-5 (2×10^3 cells/well) or SH-SY5Y (1×10^3 cells/well) in black ultra-low-attachment 96-well plates (Corning, Steuben, New York, USA), with spheroids typically forming after a 3-day culture.[33]

Antibodies and ADCs

MGA017, the unconjugated humanized anti-B7-H3 mAb precursor of the ADC, was produced at MacroGenics, Rockville, Maryland, USA, and conjugated to vc-seco-DUBA at Byondis, the Netherlands, to form vobra duo. SYD988, an anti-CD20 vc-seco DUBA ADC and the free payload, SYD978 were also provided by Byondis.

Evaluation of B7-H3 expression

Surface expression of B7-H3 was determined by flow cytometry analysis on a Gallios Flow Cytometer (Beckman Coulter). Briefly, cells (4×10^5/tube) were washed with phosphate-buffered saline (PBS) (2 mM EDTA, 1% FBS) and then incubated with PE-conjugated mouse IgG1 anti-B7-H3 mAb (BioLegend, San Diego, California, USA) at a final concentration of 1 µg/mL in a staining volume of

100 μL for 20 min at 4°C. Cells were also stained with a PE-conjugated isotype matched mAb, as control. Cells were then washed with PBS, (2 mM EDTA, 1% FBS) and the mean fluorescence intensity (MFI) of the B7-H3 positive (B7-H3^{pos}) population collected. The expression of B7-H3 was reported as mean ratio fluorescence intensity (MRFI), defined as the ratio of the MFI of cells labeled with the PE-conjugated anti-B7-H3 mAb over the MFI of cells stained with a PE-conjugated isotype-matched control mAb. The Alexa Fluor 647-conjugated MGA017, the mAb precursor of the ADC at a final concentration of 1 μg/mL, was also used to characterize B7-H3 expression by NB cell lines.

Cytotoxicity assays
Cell lines were seeded in 96-well plates (1–10×10^3 cells/well) and treated on the day after seeding with vobra duo (MacroGenics) continuously for 5–7 days or for a 2-hour pulse followed by medium removal and replacement with fresh complete medium for additional 5 or 7 days of incubation. MCTS of IMR-32, HTLA-230, LAN-5 and SH-SY5Y were also treated with vobra duo, continuously for 7 days. Daudi, IMR-32, and SH-SY5Ycells were treated with the control anti-CD20 ADC (SYD988) for 7 days. In some experiments, the free payload, SYD978, was also used. In these experiments, SYD978 was administered at concentrations corresponding to the molar amount delivered by vobra duo in the concentration range between 40 and 640 ng/mL. Each experimental condition was carried out in quadruplicate wells. Monolayer-cultured cell viability was determined by the MTS colorimetric assay, according to the manufacturer's instructions (CellTiter 96 Aqueous One Solution Cell Proliferation Assay, Promega Italia, Milano, Italy). The optical density (OD) of colored formazan produced by viable cells was analyzed on a GloMax Discover (Promega) microplate reader. Viability of MCTS was assessed by the CellTiter-Glo 3D Cell Viability Assay (Promega) and recorded as relative luminescence units (RLU) on the GloMax Discover instrument. For the luc-transduced cells NX-S2-luc, viability was determined by adding 15 μg/mL beetle luciferin (Promega) followed by the determination of RLU on the GloMax Discover instrument.

Apoptosis assay
Apoptotic cell death was evaluated by using the annexin V-FITC kit from Beckman Coulter (Brea, California, USA), following the manufacturer's instructions. In some experiments, cells were pretreated with the pan-caspases inhibitor Q-VD-OPh (Sigma-Aldrich, St. Louis, Missouri, USA) at 30 μM concentration for 30 min.

NB mouse models
Female athymic nude-Foxn1^{nu} (nu/nu) mice (Envigo, Bresso, Italy) were housed under specific pathogen-free conditions. In accordance with the "3Rs policy", experiments were reviewed and approved by the Animal Welfare Body (OPBA) of IRCCS Ospedale Policlinico San Martino and by the Italian Ministry of Health (n. 883/2020-PR). For orthotopic models, IMR-32-luc, HTLA-230-luc, LAN-5-luc, SH-SY5Y-luc, SK-N-BE2c-luc, NB-1691-luc, or NX-S2-luc cells (1×10^6 cells in 10 μL of culture medium) were inoculated in the left adrenal gland of 5 week-old mice, as described.[27–29 34 35] All mice survived surgery. For the tumor resection model, IMR-32-luc cells were inoculated in the left adrenal gland of 5 week-old mice as described above, followed by surgical resection of the primary tumor mass on day 14 in half of the mice, as previously reported.[29 36] This model was used to visualize the response of minimal residual disease to therapy after surgical resection of the primary mass. In the pseudometastatic model, HTLA-230 cells (4×10^6 cells in 200 μL culture medium) were inoculated in the tail vein of 4 week-old mice, as described.[37] Mice were randomly assigned to different arms and treated intravenously with test articles or PBS as controls.

Seven days and 4 hours after NB tumor cell inoculation in orthotopic and pseudometastatic models, respectively, mice were randomly assigned to different arms and treated with test or control articles. In orthotopic models, bio-luminescent imaging (Lumina-II, Caliper Life Sciences, Hopkinton, Massachusetts, USA) was quantified by photon counting of the tumor region of interest (ROI) followed by comparison of pre treatment and post treatment scans. Survival was ascertained by a humane endpoint. If signs of discomfort or poor health arose (eg, abdominal dilatation, dehydration, paraplegia, >15% weight loss) mice were sacrificed by CO_2 inhalation. The day of euthanasia was recorded as the day of death. In all models, mouse body weight and general physical status were recorded weekly and 24 hours before and after each treatment.

Toxicology experiments were conducted in orthotopically implanted tumor-bearing mice. Twenty-four hours after treatments, mice were anesthetized with xylazine (Xilor 2%, Bio98 Srl, Milan, Italy) and blood collected as previously reported.[38 39] Hematological levels of red blood cells, hematocrit, mean corpuscular hemoglobin (MCH), reticulocytes, hemoglobin, mean cell volume, MCH concentration, red blood cell distribution width, white blood cells and platelets were quantified. Clinical chemistry levels of serum albumin, phosphatase alkaline, glutamic-pyruvic transaminase, glutamic oxaloacetic transaminase, cholinesterase, creatine phosphokinase, lactate dehydrogenase, urea and uric acid were also quantified. All the analyses were performed at the Mouse Clinic of the IRCCS Ospedale San Raffaele (Milano, Italy).

Statistics
All in vitro experiments were performed at least three times. Differential findings among the experimental conditions were determined by one-way analysis of variance, with Tukey's multiple comparison test, using GraphPad Prism V.5 (GraphPad Software, San Diego, California, USA). Survival curves were drawn as Kaplan-Meier Cumulative Proportion Surviving graphs and

corresponding p values were calculated by using the log-rank (Mantel-Cox) test. Asterisks indicate the following p value ranges: *p<0.05, **p<0.01, ***p<0.001.

RESULTS

B7-H3 expression by human NB cell lines

To confirm the reported expression of B7-H3 in NB,[6] a panel of cell lines covering the broad genetic and phenotypic heterogeneity of the disease[4] was analyzed by flow cytometry. All human NB cell lines tested expressed B7-H3 (figure 1A and online supplemental figure S1) in a unimodal fashion, with an MRFI over control cells, stained with an isotype matched control Ab, between 20 and 70 (figure 1A). Overlapping results were also obtained by the use of MGA017 (online supplemental figure S1). The murine NB cell lines, NX-S2 and Neuro2a, did not react with anti-human B7-H3 (figure 1A and online supplemental figure S1), owing to lack of cross-reactivity of the anti-human B7-H3 mAb with the murine homologue[24] or lack of B7-H3 expression.[19]

Vobra duo demonstrates cytotoxic activity against human NB cell lines in vitro

The cytotoxic activity of vobra duo was evaluated in vitro on a panel of human NB cell lines, with a dose-dependent and time-dependent reduction in cell viability observed on continuous exposure (figure 1B and online supplemental figure S2A). A 2-hour pulse treatment, intended to mimic the short C_{max}-related exposure typically observed following intravenously administered ADCs, maintained a cytotoxic effect against all the NB cell lines analyzed, although of lesser magnitude compared with continuous treatment (figure 1B and online supplemental figure S2A). The IC50 values calculated after 7 days of incubation ranged between 37.9 and 337.8 ng/mL (0.25–2.2 nM) following the 2-hour pulse treatment and between 5.1 and 53.9 ng/mL (30–350 pM) under continuous treatment, respectively (figure 1B). Experiments performed by treating IMR-32, SH-SY5Y, and SK-N-BE2c with the free payload, SYD978, at concentrations consistent with those delivered by the ADC show a similar pattern of differential sensitivity among cell lines as with the ADC. These data suggest that the different responses to vobra duo treatment of the various NB cell lines, particularly evident in the 2-hour pulse schedule, is due to differential sensitivity to the payload (online supplemental figure S2B). Vobra duo showed a similar cytotoxic effect against a luc-expressing NB cell line, IMR-32-luc (online supplemental figure S3A), demonstrating the suitability of the luc-transduced line for further characterization of the ADC.

Vobra duo was also tested in a MCTS NB model, a three-dimensional tumor-like cellular organization. Vobra duo led to a dose-dependent reduction in cell viability (figure 1C), confirming the results obtained in monolayer culture systems, although higher concentrations of vobra duo were needed to reach a 50% reduction in cell viability compared with the monolayer cultures.
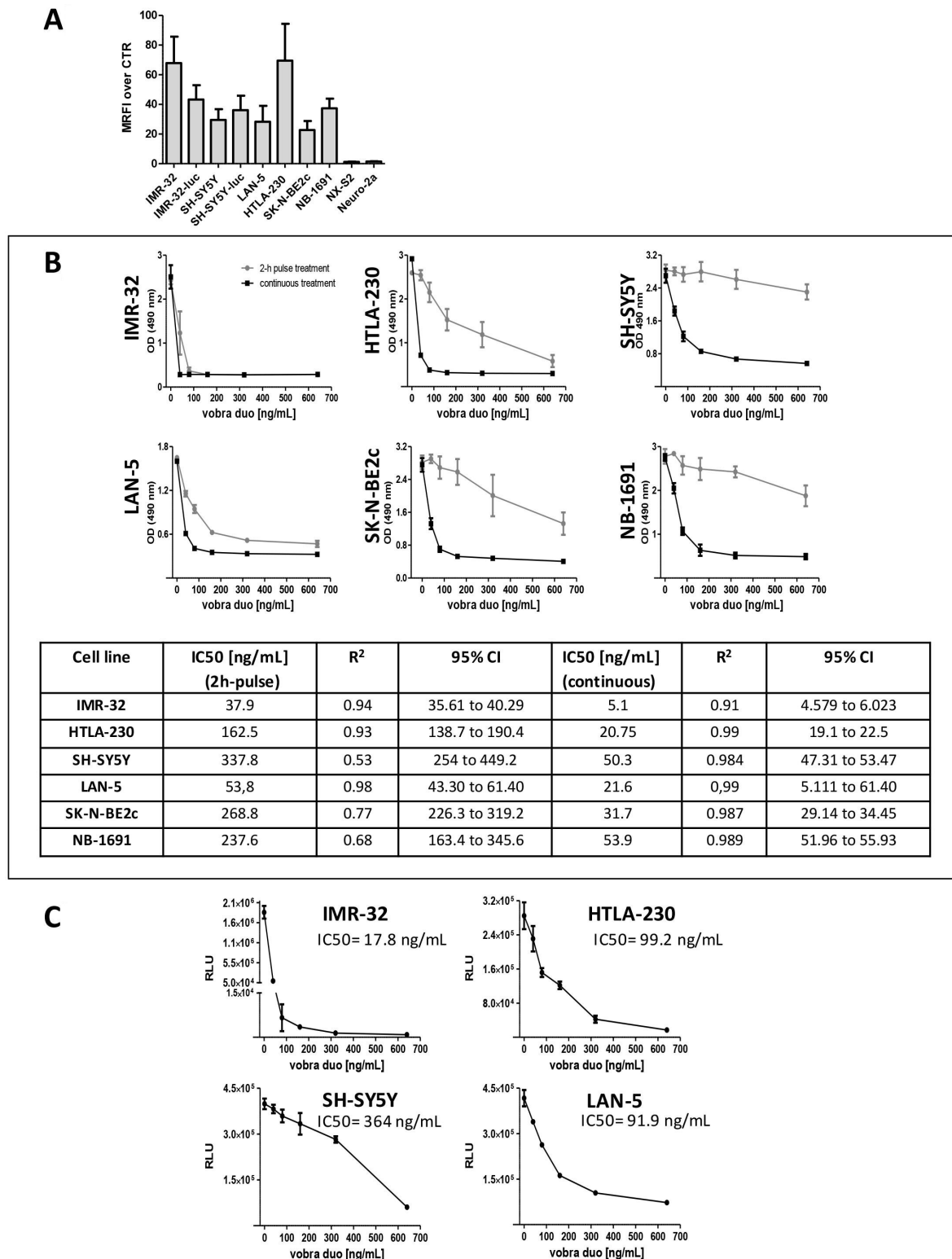
Vobra duo was inactive against NX-S2 and Daudi cell lines (online supplemental figure S3B,C). Both cell lines are unreactive to human-specific B7-H3 mAb (figure 1A, online supplemental figure S1 and S3D) and represent suitable negative controls to demonstrate the specificity of vobra duo tumor cell killing via targeting B7-H3. Daudi cells express the CD20 antigen (online supplemental figure S3D) and were killed in a dose-dependent manner by an anti-CD20 ADC carrying the same payload as vobra duo (SYD988; online supplemental figure S3D), demonstrating the susceptibility of the cell line to duocarmycin and further supporting the strict dependency on B7-H3 expression for vobra duo cytotoxic activity. The lack of effectiveness of the anti-CD20 ADC, SYD988, toward IMR-32 and SH-SY5Y cell lines that do not express CD20 further supported the specificity of the anti-B7-H3 ADC (online supplemental figure S3E,F).

Vobra duo induces dose-dependent progression from apoptotic to necrotic cell death in vitro

To evaluate the mechanism of action of vobra duo, the induction of apoptotic or necrotic cell death was investigated with the IMR-32 and SH-SY5Y cell lines. Apoptotic cell death in IMR-32 cells was observed with increasing concentrations of vobra duo, reaching a peak at 80 ng/mL, followed by continuous progression to necrosis at higher concentrations, accompanied by a decrease in the fraction of apoptotic cells (figure 2A). In contrast, vobra duo treatment induced a progressive dose-dependent increase in apoptosis of SH-SY5Y cells at all concentrations tested, accompanied by a continuous increase in necrosis of more modest degree than that observed with IMR-32 cells (figure 2B). Pretreatment with the pan-caspase inhibitor, Q-VD-OPh, reverted the induction of apoptosis (online supplemental figure S4A,B), confirming that vobra duo mediates cytotoxicity by an apoptotic mechanism.

Vobra duo can exert bystander cell killing of B7-H3-negative cells

To evaluate the bystander cell killing effect of vobra duo, B7-H3-unreactive murine NB NX-S2-luc cells were co-cultured at different ratios with the human B7-H3-positive NB cell lines, IMR-32, HTLA-230, and SH-SY5Y. As demonstrated in figure 2C–E, the cell viability of the B7-H3-unreactive cells progressively decreased as the relative abundance of co-cultured B7-H3-positive cells increased, consistent with bystander cytotoxicity. As expected, the reduction of NX-S2-luc cell viability mediated by the bystander effect reflected the sensitivity of the susceptible cell lines to vobra duo treatment. IMR-32 and HTLA-230 cell lines, which are more sensitive to vobra duo treatment compared with SH-SY5Y (IMR-32 IC50=5.1 ng/mL, HTLA-230 IC50=20.75 ng/mL, SH-SY5Y IC50=50.3 ng/mL), resulted in significant bystander activity at low cell-to-cell ratio, while higher ratios were needed in the case of SH-SY5Y cells (figure 2C–E).

Cell line	IC50 [ng/mL] (2h-pulse)	R^2	95% CI	IC50 [ng/mL] (continuous)	R^2	95% CI
IMR-32	37.9	0.94	35.61 to 40.29	5.1	0.91	4.579 to 6.023
HTLA-230	162.5	0.93	138.7 to 190.4	20.75	0.99	19.1 to 22.5
SH-SY5Y	337.8	0.53	254 to 449.2	50.3	0.984	47.31 to 53.47
LAN-5	53,8	0.98	43.30 to 61.40	21.6	0,99	5.111 to 61.40
SK-N-BE2c	268.8	0.77	226.3 to 319.2	31.7	0.987	29.14 to 34.45
NB-1691	237.6	0.68	163.4 to 345.6	53.9	0.989	51.96 to 55.93

Figure 1 Cytotoxic activity of vobra duo against a panel of human B7-H3 positive NB cell lines. (A) The histograms represent the expression of human B7-H3 by human and murine NB cell lines. Protein expression was evaluated by flow cytometry and is expressed as mean ratio fluorescence intensity (MRFI) of positive labeled cells over cells stained with an isotype matched control Ab. (B) NB cell lines were treated with escalating concentrations of vobra duo (40-80-160-320-640 ng/mL) continuously for 7 days (black square) or for a 2-hour pulse followed by a washing step and continued incubation (gray circles). Viability was assessed by the MTS assay. Data are expressed as mean±SD. Vobra duo cytotoxicity IC50, calculated for both treatment schedules is reported. (C) Multicellular tumor spheroids models of four different NB cell lines were treated with increasing concentrations of vobra duo (40, 80, 160, 320, 640 ng/mL) for 7 days. Cell viability was determined by the Cell Titer Glo 3D Cell Viability Assay. Data are expressed as mean±SD. Ab, antibody; NB, neuroblastoma; MTS, water-soluble tetrazolium salt; OD, optical density; RLU, relative luminescence intensity; vobra duo, vobramitamab duocarmazine.
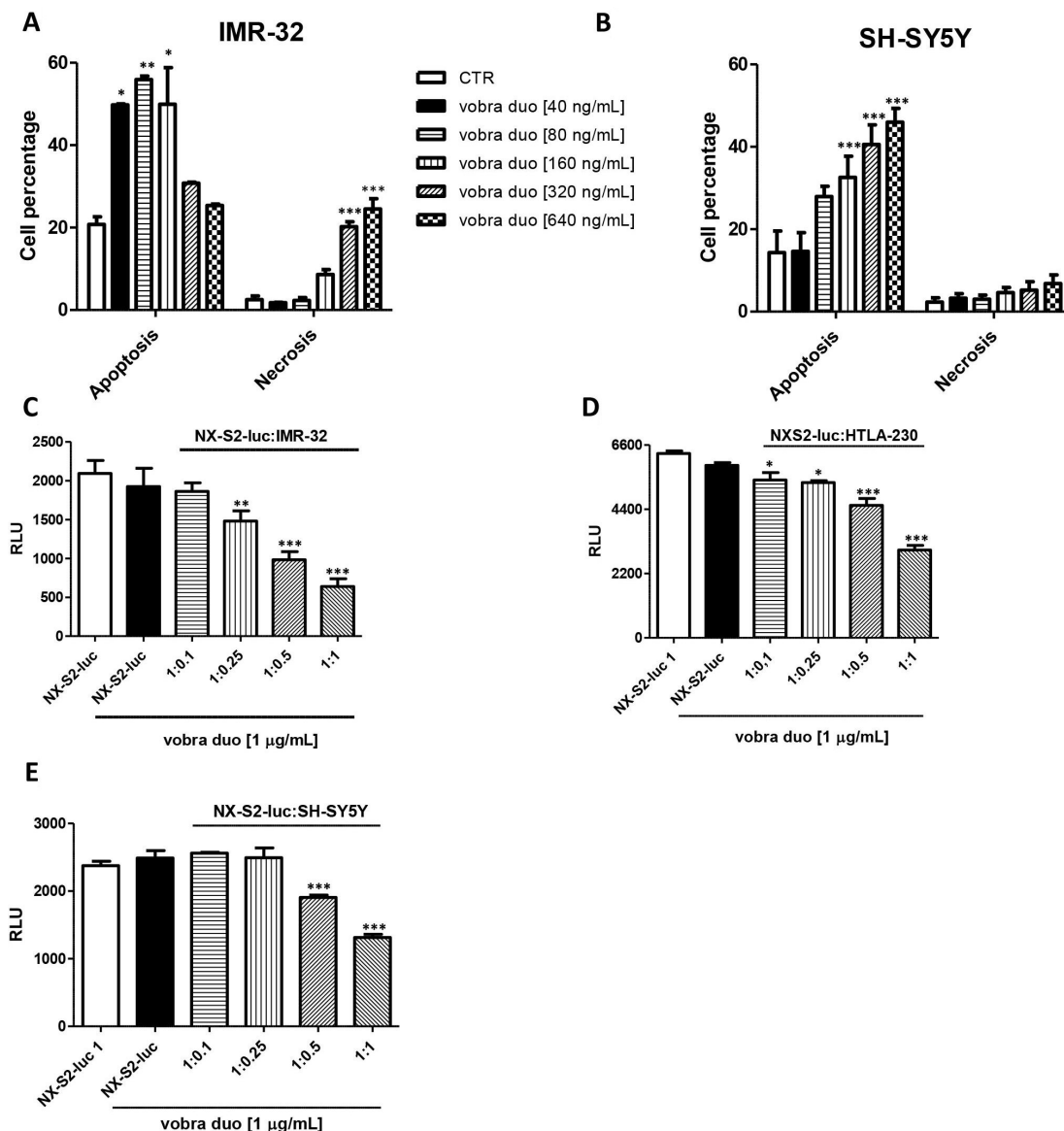
Figure 2 Vobra duo induces apoptotic and necrotic cell death and mediates bystander cell killing. (A, B) IMR-32 and SH-SY5Y cells were seeded in 6-well plates (4.5×10^5 cells/well). The day after seeding, cells were treated with vobra duo for 24 hours, harvested and processed for the detection of apoptosis or necrosis. The percentage of apoptosis and necrosis induced by vobra duo is indicated as mean±SD. (C–E) Human B7-H3-negative NX-S2-luc cells (4×10^3 cells/well) were co-cultured in black 96-well plates at different ratio (1:0.1, 1:0.25, 1:0.5 and 1:1) with IMR-32, HTLA-230, or SH-SY5Y cells and treated with vobra duo at the concentration of 1 µg/mL for 5 days. The graph represents the viability of NX-S2-luc cells expressed as relative luminescence unit (RLU, mean±SD). luc, luciferase; vobra duo, vobramitamab duocarmazine.

Antitumor activity of vobra duo in in vivo NB mouse models

The antitumor efficacy of vobra duo was evaluated in mouse models of NB disease in comparison to or in combination with standard-of-care therapy. Orthotopic, pseudometastatic, and tumor-resected models were used, conditions aimed at recapitulating primary tumor growth (including relapsed/refractory NB), metastatic disease, and minimal residual disease (MRD), respectively.[27–30 35 37]

Vobra duo's activity was evaluated in several orthotopic NB animal models by monitoring the tumor growth of luc-transduced NB cell lines via bio-luminescence imaging (BLI), as well as survival to humane endpoint sacrifice. Following NB cells inoculation, mice with established

tumors were randomly assigned to two treatment groups and administered PBS or 1 mg/kg vobra duo intravenously one time a week for 3 weeks (QWx3). Vobra duo showed activity in all human NB models tested, leading to tumor growth delay and significant increases in survival relative to vehicle-treated mice (figure 3A–E). No activity was observed with the murine NX-S2-luc model, which is not targeted by the ADC (figure 3F). Vobra duo QWx3 was effective also in a pseudometastatic model compared with control animals (figure 3G).

The role, if any, played by the naked anti-B7-H3 antibody precursor, MGA017, or the payload in the form of an irrelevant (anti-CD20) duocarmycin-based ADC (SYD988) compared
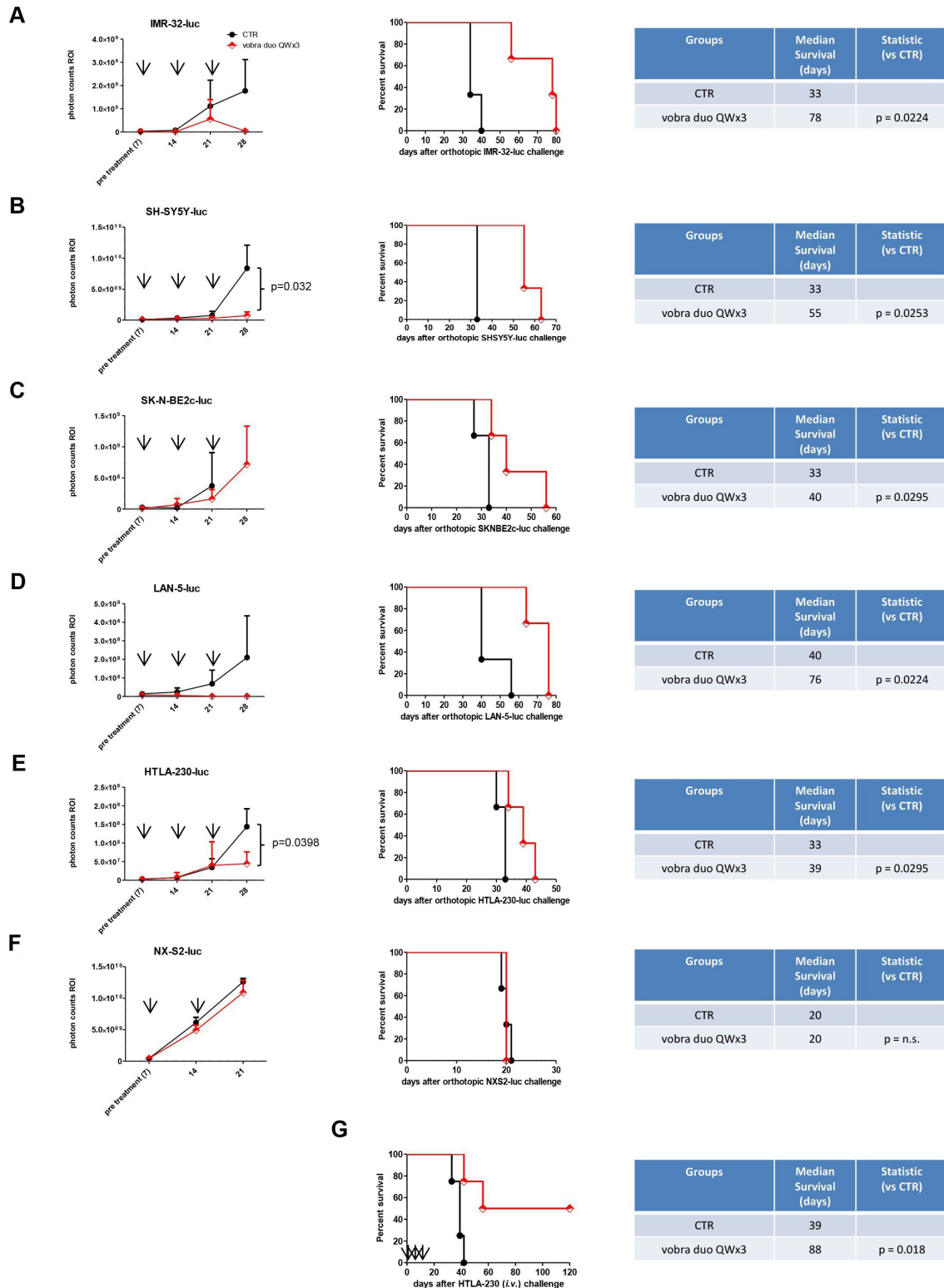
Figure 3 Antitumor effects of vobra duo in orthotopic and pseudometastatic murine models of NB. Mice, 7 days (A–F) or 4 hours (G) after being inoculated with NB cells, were randomly assigned to two treatment groups and intravenously treated with PBS (CTR) or 1 mg/kg vobra duo once a week for 3 weeks (vobra duo QWx3). (A–F) BLI curves and survival in luciferase (luc)-transfected human (A–E) and murine (F) orthotopic NB models (n=3 mice/group). For each cell line injected, tumor growth was monitored by BLI (left panels). Photon counts in the tumor region of interest (ROI) are reported at pre treatment and 7 days post treatment. X axes show the days after tumor cells injection. Results are presented as mean±SEM, with comparison of vobra duo versus CTR reported when statistically significant. Survival curves and statistical comparison of vobra duo QWx3 versus CTR are shown. (G) Survival in the pseudometastatic model (n=4 mice/group). Statistical comparison of vobra duo QWx3 versus CTR is reported. Arrow: treatment (T). BLI, bio-luminescence imaging; i.v., intravenous; NB, neuroblastoma; PBS, phosphate-buffered saline; QWx3, one time a week for 3 weeks; vobra duo, vobramitamab duocarmazine.
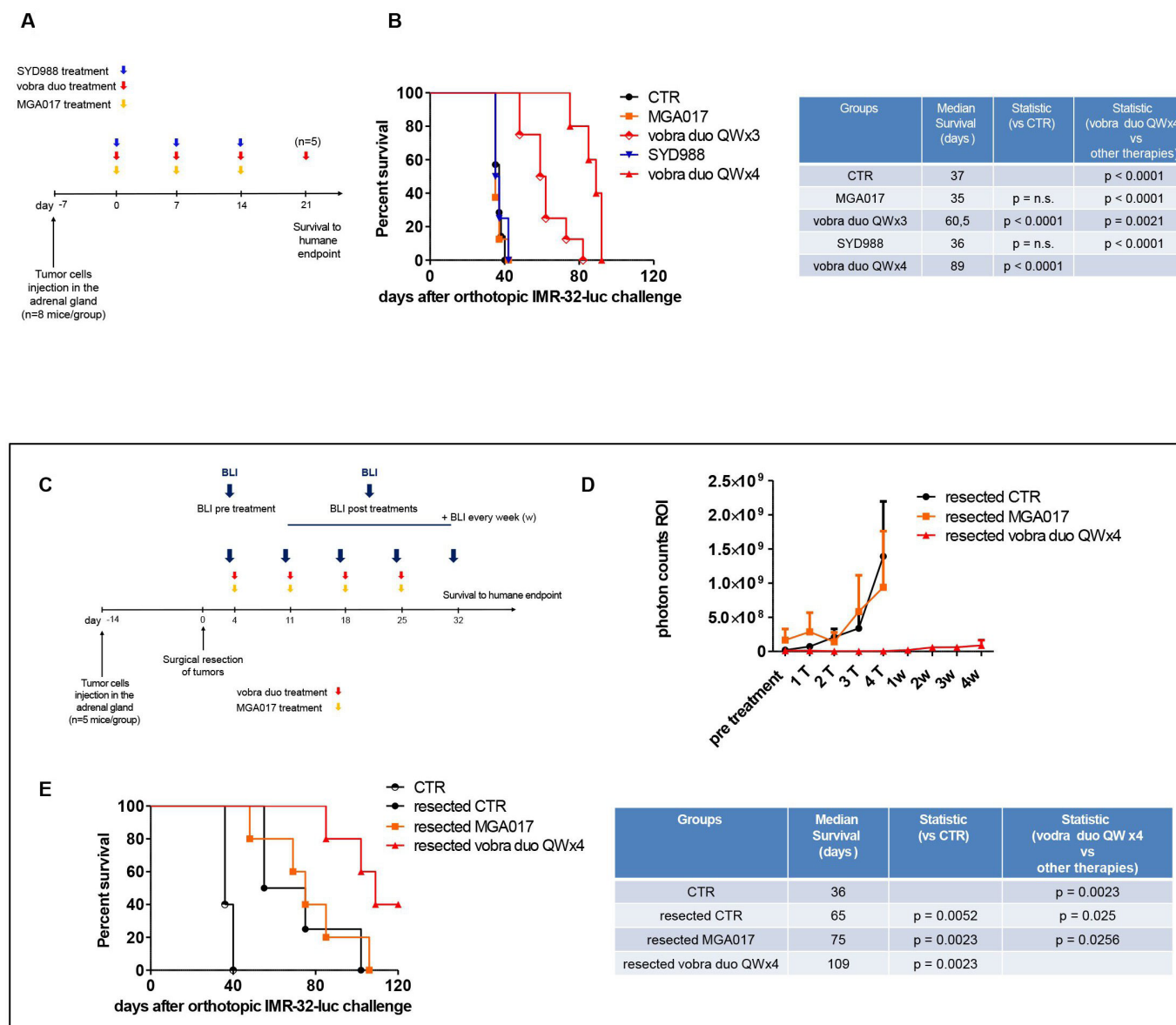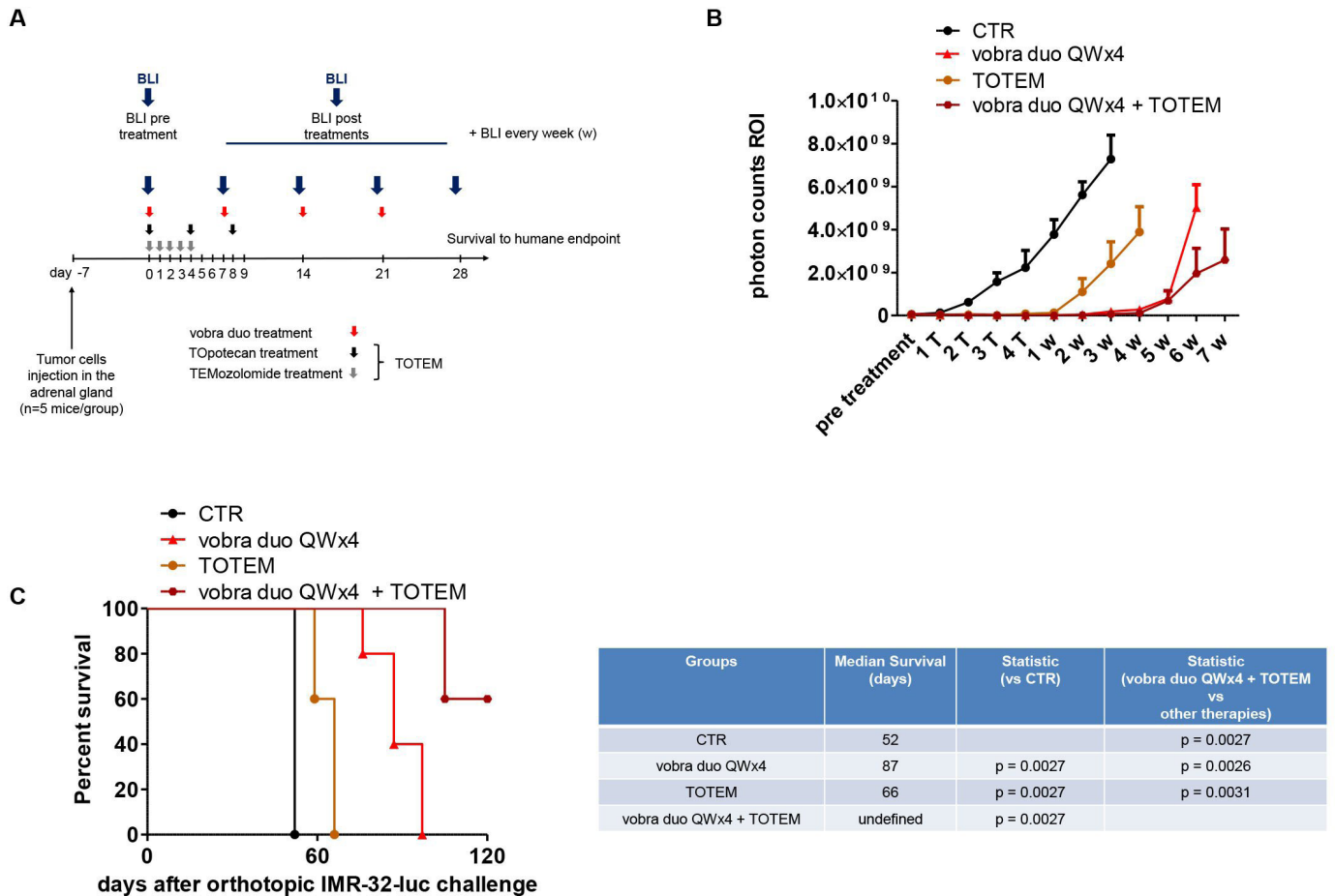
Figure 4 Vobra duo therapeutic efficacy in an orthotopic and in a primary tumor-resected model of NB. (A) Schematic and timeline of the experiment. IMR-32-luc cells were orthotopically inoculated in the mouse left adrenal gland. Treatments (MGA017, vobra duo QWx3, SYD988, vobra duo QWx4) started 7 days post cell inoculation and were performed as reported in the Results section. (B) Survival in NB-bearing mice treated with either vobra duo QWx3 (n=8 mice) or vobra duo QWx4 (n=5 mice). Statistics (vobra duo QWx3, MGA017 and SYD988 vs CTR; vobra duo QWx4 vs all groups) are reported. (C) Schematic and timelines of the experiment. IMR-32-luc cells were orthotopically inoculated in the mouse left adrenal gland. Tumors were surgically resected 2 weeks after, and treatments (n=5 mice/group) started 4 days post tumor resection, as reported. Untreated, control mice (CTR) received PBS. (D) Tumor growth was monitored by BLI. Photon counts in the tumor region of interest (ROI) are reported at pretreatment and 7 days post each treatment (T) and for the subsequent 4 weeks (w). Results are presented as mean±SEM. (E) Kaplan-Meier survival curves with corresponding statistical analysis comparing all therapeutic groups with vobra duo QWx4 are shown. CTR: mice orthotopically injected with tumor cells, and that did not undergo tumor surgical resection. BLI, bio-luminescence imaging; luc, luciferase; NB, neuroblastoma; QWx3, one time a week for 3 weeks; QWx4, one time a week for 4 weeks; vobra duo, vobramitamab duocarmazine.

with that of vobra duo in mediating antitumor activity was investigated in IMR-32-luc cell-bearing mice (figure 4A). Vobra duo 1 mg/kg QWx3 increased survival compared with untreated mice, while all other treatments were indistinguishable from vehicle-treated mice (figure 4B). Increasing vobra duo exposure to QWx4 further improved survival compared with mice treated QWx3. Importantly, no weight loss was

evidenced in any of the treatment groups, including in mice treated with vobra duo QWx4 (online supplemental figure S5). This latter multidose regimen (vobra duo QWx4) was therefore used in subsequent experiments.

The effect of vobra duo was next assessed on MRD by using a NB tumor resection model whereby the primary tumor mass was surgically removed 2 weeks following the implantation

A

B

C

Groups	Median Survival (days)	Statistic (vs CTR)	Statistic (vobra duo QWx4 + TOTEM vs other therapies)
CTR	52		p = 0.0027
vobra duo QWx4	87	p = 0.0027	p = 0.0026
TOTEM	66	p = 0.0027	p = 0.0031
vobra duo QWx4 + TOTEM	undefined	p = 0.0027	

Figure 5 Treatment combination of vobra duo and TOTEM in an orthotopic model of NB. (A) Schematic and timelines of the in vivo experiments. IMR-32-luc cells were orthotopically inoculated in the left adrenal gland of mice. Treatments (n=5 mice/group; vobra duo QWx4, TOTEM, vobra duo QWx4+TOTEM) started 7 days post cell inoculation and were performed as reported. Untreated, control mice (CTR) received PBS. (B) Tumor growth monitored by BLI. Photon counts in the tumor region of interest (ROI) are reported at pretreatment, 7 days post each treatment (T) and for the subsequent 7 weeks (w). Results are presented as mean±SEM. (C) Kaplan-Meier survival curves with corresponding statistical analysis comparing all therapeutic groups with vobra duo QWx4 are shown. BLI, bio-luminescence imaging; luc, luciferase; NB, neuroblastoma; PBS, phosphate-buffered saline; QWx4, one time a week for 4 weeks; vobra duo, vobramitamab duocarmazine.

in the adrenal gland (figure 4C). Treatment of NB-resected mice with vobra duo QWx4 led to a significant delay in tumor regrowth, as shown by BLI imaging (figure 4D) and increased survival (figure 4E), while MGA017 was ineffective.

The combination of TOpotecan and TEMozolomide (TOTEM) is standard-of-care therapy for relapsed NB[40 41]; it was therefore of interest to ascertain the activity of vobra duo in comparison and in combination with TOTEM. Both primary orthotopic and MRD tumor models were used in IMR-32-luc-bearing mice treated with vobra duo (1 mg/kg QWx4), TOTEM (topotecan intraperitoneally 10 mg/kg Q4D×3 and temozolomide oral gavage 34 mg/kg QDx5) or both (figures 5A and 6A). In mice bearing an established orthotopically implanted tumor, TOTEM administration slowed tumor growth and increased survival compared with untreated mice (figure 5B,C). Vobra duo QWx4 alone, however, was superior to TOTEM in controlling tumor growth and increasing mouse survival. The addition of TOTEM to vobra duo QWx4 further delayed tumor growth and increased survival, with three of five mice remaining alive for 120 days

following tumor cells implantation (figure 5B,C). In the resected tumor model, post-surgical treatment with TOTEM or vobra duo QWx4 transiently arrested tumor growth and equally improved survival compared with resected untreated mice (figure 6B,C). However, the combination of vobra duo QWx4 and TOTEM further delayed tumor growth and increased survival, with six out of eight mice alive 120 days after tumor cells injection (figure 6B,C).

Further regimen optimization was investigated by assessing the responses to repeated cycles of treatment with vobra duo QWx4 in the relapsed NB mouse model (figure 7A). Mice bearing established, orthotopically implanted IMR-32-luc tumors were treated with vobra duo QWx4, resulting in tumor growth inhibition and increased survival compared with untreated mice (figure 7B,C). Two weeks after the end of the first treatment cycle, vobra duo-treated animals whose tumor grew back were retreated with vobra duo (QWx4, two cycles), resulting in tumor growth arrest, a decrease in tumor volume (figure 7B), and increased survival compared with animals that received a single cycle of vobra duo (figure 7C).
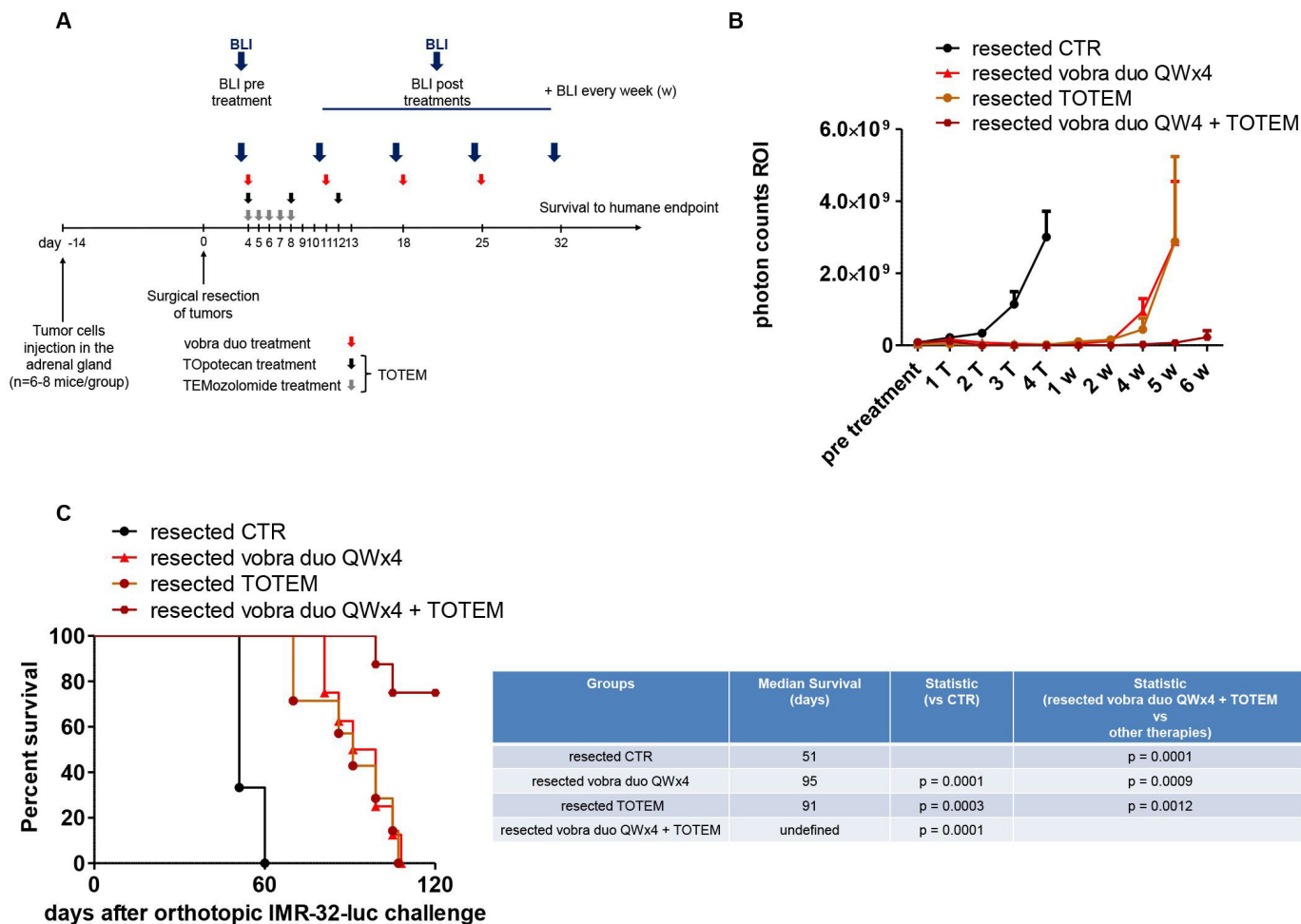
Figure 6 Treatment combination of vobra duo and TOTEM in a primary tumor-resected model of NB. (A) Schematic and timeline of the in vivo experiments. IMR-32-luc cells were orthotopically inoculated in the left adrenal gland of mice. Tumors were surgically resected 2 weeks after, and treatments (n=5, CTR mice, n=8, treatments groups) started 4 days post tumor resection, as reported (vobra duo QWx4, TOTEM, vobra duo QWx4+TOTEM). Untreated, control mice (CTR) received PBS. (B) Tumor growth monitored by BLI. Photon counts in the tumor region of interest (ROI) are reported at pretreatment, 7 days post each treatment (T) and for the subsequent 6 weeks (w). Results are presented as mean±SEM. (C) Kaplan-Meier survival curves with corresponding statistical analysis comparing all therapeutic groups with vobra duo QWx4 are shown. BLI, bioluminescence imaging; luc, luciferase; NB, neuroblastoma; PBS, phosphate-buffered saline; QWx4, one time a week for 4 weeks; vobra duo, vobramitamab duocarmazine.

When tumors grew back again following the second cycle, a third cycle of vobra duo (QWx4, three cycles) was still capable of controlling tumor growth (figure 7B) and further increasing survival, with all mice being alive 120 days post tumor implantation (figure 7C). Repeat cycles of vobra duo were superior to TOTEM chemotherapy in the orthotopic NB model (online supplemental figure S6). No evidence of hematological toxicity (online supplemental figure S7A,B) or clinical chemistry alterations (online supplemental figure S8) were observed in treated mice, including those subjected to multiple cycles of vobra duo.

DISCUSSION

Responsible for 15% of childhood cancer deaths,[1] NB continues to be a significant unmet medical need. While aggressive chemotherapy remains the backbone of medical intervention, chemotherapy-associated toxicity and the development of drug resistance are persistent major obstacles to achieving durable clinical success, particularly in high-risk patients.[4 42 43] Endowed with the selective targeting ability of mAbs and the cytotoxic potency of chemotherapeutics, ADCs have emerged as an immune intervention with the potential for enhancing the chemotherapeutic window by reducing the undesirable systemic toxicity of the payload via tumor-specific targeting. In this study, we provide evidence of antitumor activity in several preclinical NB models of the investigational ADC, vobra duo, a humanized anti-B7-H3 IgG1 mAb conjugated via a cleavable linker to a novel duocarmycin-based payload.

At the end of 2022, 12 ADCs have been approved by the FDA for the treatment of hematological malignancies or solid tumors in adults.[44] Application of ADCs to pediatric tumors, however, remains under-represented, with the only exception of gemtuzumab ozogamicin (Mylotarg),
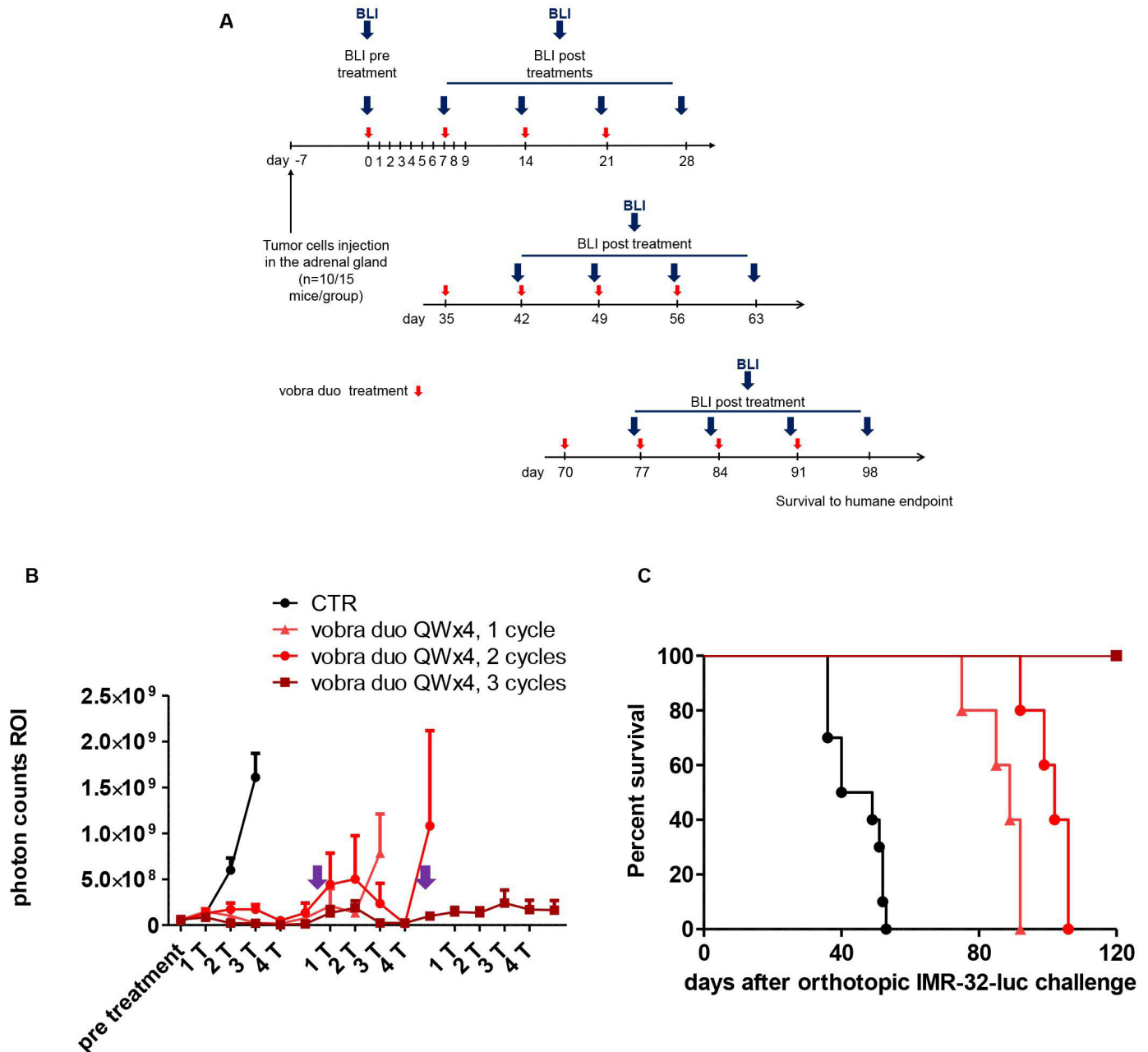
Figure 7 Repeated vobra duo treatment in a relapsed model of NB. (A) Schematic and timelines of the in vivo experiments. IMR-32-luc cells were orthotopically inoculated in the left adrenal gland of mice (n=10, CTR mice, n=15, vobra duo QWx4 treatment group). Vobra duo QWx4, 1 cycle treatment started 7 days post cell inoculation. Mice were re-treated with vobra duo QWx4 (vobra duo QWx4, 2 cycles, n=10 and vobra duo QWx4, 3 cycles, n=5, respectively) when BLI imaging showed tumor relapse (purple arrow). Untreated, control mice (CTR) received PBS. (B) Tumor growth monitored by BLI. Photon counts in the tumor region of interest (ROI) are reported at pretreatment and 7 days post treatments (T) of each course. Results are presented as mean±SEM. (C) Kaplan-Meyer survival curves of untreated (CTR) mice, vobra duo QWx4, two cycles and three cycles vobra duo QWx4, are presented. Statistics: single and repeated vobra duo QWx4, versus CTR, p=0.0005; vobra duo QWx4, two cycles versus vobra duo QWx4, p=0.0082; vobra duo QWx4, three cycles versus vobra duo QWx4, two cycles, p=0.0027. BLI, bio-luminescence imaging; luc, luciferase; NB, neuroblastoma; PBS, phosphate-buffered saline; QWx4, one time a week for 4 weeks; vobra duo, vobramitamab duocarmazine.

which has been recently approved for the treatment of newly diagnosed CD33-positive acute myeloid leukemia of both adult and pediatric patients aged 1 month and older.[44] In recent years, several experimental ADCs have been developed for the potential treatment of NB, attesting to the growing interest in exploring this modality

to address this unmet medical need. These include ADCs targeting GD2,[45] GPC2,[46] the vesicular LGALS3BP protein,[38] ALK,[47] and B7-H3.[48]

B7-H3 has been reported to be broadly and frequently expressed in cancers of both the adults and children.[6–9] In NB, expression was confirmed in primary tumors,

tumor cell lines, and bone marrow (BM)-infiltrating NB cells.[6 10 34 48 49] As previously reported, B7-H3 expression in BM-infiltrating NB cells does not always overlap with GD2 expression, with variants characterized by low and/ or negative GD2 expression displaying robust B7-H3 staining, as reported by us (reference[34] and data not shown) and others[49]; hence, B7-H3 targeting may expand the range of interventions in NB.

B7-H3 has been widely investigated as a target for various immunotherapeutic approaches, including humanized Fc-engineered mAbs, radioimmunotherapy, CAR-T cells, and ADCs.[19] In the case of chemotherapy-sensitive cancers, such as NB, the ADC approach may provide the greatest opportunity to improve outcome by combining an established mechanism of action with the potential for increased tolerability compared with systemic therapy.

In this report, we have addressed the antitumor potential of a novel anti-B7-H3 ADC, vobra duo, in NB by subjecting it to multiple in vitro and in vivo challenges. Multiple cell culture models were analyzed, including the MCTS model, a culture system that displays a complexity intermediate between two-dimensional cell cultures and in vivo tumors.[50 51] MCTS approximates the complex architecture and physiology of a solid tumor mass, including mimicry of the differential access to oxygen, nutrients, and drugs by the different layers of the tumor, and therefore carrying greater predictive value for response to treatment than standard cultures.[50 51] The enhanced requirement of this model translated into vobra duo IC50 values that were higher than those obtained in the monolayer cell culture system; yet, with values still in the nanomolar range, vobra duo is predicted to span a targeted therapeutic range consistent with that of other ADCs. Furthermore, bystander cell killing by vobra duo was observed against B7-H3-unreactive murine NB cells, consistent with a prior observation[24] and implying potential benefit in the treatment of tumors with heterogeneous antigen expression.

Clinically relevant NB mouse models that recapitulated primary tumor growth, circulating tumor cells and metastatic disease, as well as minimal residual disease and tumor relapse, all contributed to validating the antitumor activity of vobra duo in vivo. A treatment schedule consisting of 3 weekly intravenous doses of 1 mg/kg of vobra duo was effective in five different orthotopic mouse models developed via tumor cell implantation in the adrenal gland, demonstrating that vobra duo can kill tumor cells in an established tumor mass. Administration of the parental unconjugated anti-B7-H3 mAb or an irrelevant mAb with the same payload was ineffective, demonstrating the potency and specificity of the ADC in these model systems. In a pseudometastatic tumor model, developed via tumor cell tail vein injection, vobra duo resulted in a significant increase in the survival of treated mice compared with controls. Interestingly, increasing the weekly doses of 1 mg/kg from three to four consecutive weeks of dosing was associated with a further improved tumor response and was equally well tolerated, suggesting that dose-optimization and regimen-optimization strategies could further enhance vobra duo clinical activity.

Patients with NB often undergo surgical debulking, particularly in intermediate-risk and high-risk disease.[43] To reflect this clinical practice, vobra duo efficacy was also demonstrated in a resected mouse model of NB, in which the primary tumor mass was surgically removed 2 weeks after orthotopic implantation in the adrenal gland, supporting the ability of the ADC to address minimal residual disease.

Lastly, vobra duo was compared with the approved standard-of-care practice TOTEM combination therapy translated to animal models. The methylating agent, temozolomide, has shown activity in patients with refractory or relapsed high-risk NB[52] and its combination with either irinotecan or topotecan, inhibitors of topoisomerase I, represents the backbone therapy in relapsed NB.[53 54] TOTEM was evaluated in orthotopic and in surgically resected NB animal models and compared with vobra duo. A single course of vobra duo was as effective as TOTEM chemotherapy in controlling NB recurrence; furthermore, repeat cycles of vobra duo were superior to TOTEM chemotherapy in the orthotopic NB model. TOTEM chemotherapy is associated with significant toxicity.[54 55] Given its target selectivity, vobra duo may provide a potential alternative to systemic chemotherapy, particularly in patients with limited tolerance to aggressive treatments. Furthermore, combining TOTEM with vobra duo significantly increased animal survival compared with the single agents, suggesting that the two interventions address non-redundant cytolytic mechanisms and offering a combinatorial opportunity in suitable patients with aggressive disease.

ORCID iDs
Fabio Pastorino http://orcid.org/0000-0002-8312-808X
Mirco Ponzoni http://orcid.org/0000-0002-6164-4286

REFERENCES

1. Maris JM. Recent advances in neuroblastoma. *N Engl J Med* 2010;362:2202–11.
2. Brodeur GM. Neuroblastoma: biological insights into a clinical enigma. *Nat Rev Cancer* 2003;3:203–16.
3. Tolbert VP, Matthay KK. Neuroblastoma: clinical and biological approach to risk stratification and treatment. *Cell Tissue Res* 2018;372:195–209.
4. Matthay KK, Maris JM, Schleiermacher G, et al. Neuroblastoma. *Nat Rev Dis Primers* 2016;2:16078.
5. Cohn SL, Pearson ADJ, London WB, et al. The International neuroblastoma risk group (INRG) classification system: an INRG task force report. *J Clin Oncol* 2009;27:289–97.
6. Castriconi R, Dondero A, Augugliaro R, et al. Identification of 4Ig-B7-H3 as a neuroblastoma-associated molecule that exerts a protective role from an NK cell-mediated lysis. *Proc Natl Acad Sci U S A* 2004;101:12640–5.
7. Zhang Z, Jiang C, Liu Z, et al. B7-H3-targeted CAR-T cells exhibit potent antitumor effects on hematologic and solid tumors. *Mol Ther Oncolytics* 2020;17:180–9.
8. Maachani UB, Tosi U, Pisapia DJ, et al. B7-H3 as a Prognostic biomarker and therapeutic target in pediatric central nervous system tumors. *Transl Oncol* 2020;13:365–71.
9. Majzner RG, Theruvath JL, Nellan A, et al. CAR T cells targeting B7-H3, a pan-cancer antigen, demonstrate potent Preclinical activity against pediatric solid tumors and brain tumors. *Clin Cancer Res* 2019;25:2560–74.
10. Gregorio A, Corrias MV, Castriconi R, et al. Small round blue cell tumours: diagnostic and Prognostic usefulness of the expression of B7-H3 surface molecule. *Histopathology* 2008;53:73–80.
11. Zang X, Allison JP. The B7 family and cancer therapy: Costimulation and Coinhibition. *Clin Cancer Res* 2007;13:5271–9.
12. Hofmeyer KA, Ray A, Zang X. The contrasting role of B7-H3. *Proc Natl Acad Sci U S A* 2008;105:10277–8.
13. Wang J, Chong KK, Nakamura Y, et al. B7-H3 associated with tumor progression and epigenetic regulatory activity in cutaneous Melanoma. *J Invest Dermatol* 2013;133:2050–8.
14. Sun J, Guo Y, Li X, et al. B7-H3 expression in breast cancer and upregulation of VEGF through gene silence. *OTT* 2014;7:1979.
15. Zang X, Thompson RH, Al-Ahmadie HA, et al. B7-H3 and B7X are highly expressed in human prostate cancer and associated with disease spread and poor outcome. *Proc Natl Acad Sci U S A* 2007;104:19458–63.
16. Hu Y, Lv X, Wu Y, et al. Expression of Costimulatory molecule B7-H3 and its Prognostic implications in human acute leukemia. *Hematology* 2015;20:187–95.
17. Altan M, Pelekanou V, Schalper KA, et al. B7-H3 expression in NSCLC and its association with B7-H4, PD-L1 and tumor-infiltrating lymphocytes. *Clin Cancer Res* 2017;23:5202–9.
18. Feng R, Chen Y, Liu Y, et al. The role of B7-H3 in tumors and its potential in clinical application. *Int Immunopharmacol* 2021;101:S1567-5769(21)00789-X.
19. Kontos F, Michelakos T, Kurokawa T, et al. B7-H3: an attractive target for antibody-based Immunotherapy. *Clin Cancer Res* 2021;27:1227–35.
20. Beck A, Goetsch L, Dumontet C, et al. Strategies and challenges for the next generation of antibody–drug conjugates. *Nat Rev Drug Discov* 2017;16:315–37.
21. Giugliano F, Corti C, Tarantino P, et al. Bystander effect of antibody-drug conjugates: fact or fiction *Curr Oncol Rep* 2022;24:809–17.
22. Dan N, Setua S, Kashyap V, et al. n.d. Antibody-drug conjugates for cancer therapy: chemistry to clinical implications. *Pharmaceuticals*;11:32.
23. do Pazo C, Nawaz K, Webster RM. The oncology market for antibody-drug conjugates. *Nat Rev Drug Discov* 2021;20:583–4.
24. Scribner JA, Brown JG, Son T, et al. Preclinical development of Mgc018, a Duocarmycin-based antibody-drug conjugate targeting B7-H3 for solid cancer. *Mol Cancer Ther* 2020;19:2235–44.
25. Kurmasheva R, Mosse YP, Del Pozo V, et al. Testing of B7-H3 targeting antibody-drug conjugate (ADC) Mgc018 in models of pediatric solid tumors by the pediatric Preclinical testing consortium (PPTC). *JCO* 2021;39:10037.
26. Jang S, Powderly JD, Spira AI, et al. Phase 1 dose escalation study of Mgc018, an anti-B7-H3 antibody-drug conjugate (ADC), in patients with advanced solid tumors. *JCO* 2021;39:2631.
27. Cossu I, Bottoni G, Loi M, et al. Neuroblastoma-targeted Nanocarriers improve drug delivery and penetration, delay tumor growth and Abrogate metastatic diffusion. *Biomaterials* 2015;68:89–99.
28. Di Paolo D, Pastorino F, Brignole C, et al. Combined replenishment of miR-34A and Let-7B by targeted nanoparticles inhibits tumor growth in neuroblastoma Preclinical models. *Small* 2020;16:e1906426.
29. Pastorino F, Di Paolo D, Piccardi F, et al. Enhanced antitumor efficacy of clinical-grade vasculature-targeted liposomal doxorubicin. *Clin Cancer Res* 2008;14:7320–9.
30. Ponzoni M, Curnis F, Brignole C, et al. Enhancement of tumor homing by chemotherapy-loaded nanoparticles. *Small* 2018;14:e1802886.
31. Lode HN, Xiang R, Varki NM, et al. Targeted Interleukin-2 therapy for spontaneous neuroblastoma metastases to bone marrow. *J Natl Cancer Inst* 1997;89:1586–94.
32. Klein E, Klein G, Nadkarni JS, et al. Surface Igm-Kappa specificity on a Burkitt lymphoma cell in vivo and in derived culture lines. *Cancer Res* 1968;28:1300–10.
33. Morandi F, Bensa V, Calarco E, et al. The olive leaves extract has anti-tumor effects against neuroblastoma through inhibition of cell proliferation and induction of apoptosis. *Nutrients* 2021;13:2178.
34. Brignole C, Bensa V, Fonseca NA, et al. Cell surface Nucleolin represents a novel cellular target for neuroblastoma therapy. *J Exp Clin Cancer Res* 2021;40.
35. Pastorino F, Brignole C, Marimpietri D, et al. Vascular damage and anti-angiogenic effects of tumor vessel-targeted liposomal chemotherapy. *Cancer Res* 2003;63:7400–9.
36. Pastorino F, Marimpietri D, Brignole C, et al. Ligand-targeted liposomal therapies of neuroblastoma. *Curr Med Chem* 2007;14:3070–8.
37. Pastorino F, Brignole C, Marimpietri D, et al. Doxorubicin-loaded Fab' fragments of anti-Disialoganglioside Immunoliposomes selectively inhibit the growth and dissemination of human neuroblastoma in nude mice. *Cancer Res* 2003;63:86–92.
38. Capone E, Lamolinara A, Pastorino F, et al. Targeting vesicular Lgals3Bp by an antibody-drug conjugate as novel therapeutic strategy for neuroblastoma. *Cancers (Basel)* 2020;12:2989.
39. Corallo D, Pastorino F, Pantile M, et al. Autophagic flux inhibition enhances cytotoxicity of the receptor tyrosine kinase inhibitor Ponatinib. *J Exp Clin Cancer Res* 2020;39.
40. Pastorino F, Loi M, Sapra P, et al. Tumor regression and Curability of Preclinical neuroblastoma models by pegylated Sn38 (EZN-2208), a novel Topoisomerase I inhibitor. *Clin Cancer Res* 2010;16:4809–21.
41. Chen L, Pastorino F, Berry P, et al. Preclinical evaluation of the first intravenous small molecule Mdm2 antagonist alone and in combination with Temozolomide in neuroblastoma. *Int J Cancer* 2019;144:3146–59.
42. Wienke J, Dierselhuis MP, Tytgat GAM, et al. The immune landscape of neuroblastoma: challenges and opportunities for novel therapeutic strategies in pediatric oncology. *Eur J Cancer* 2021;144:123–50.
43. Qiu B, Matthay KK. Advancing therapy for neuroblastoma. *Nat Rev Clin Oncol* 2022;19:515–33.
44. Fu Z, Li S, Han S, et al. "Antibody drug conjugate: the "biological missile" for targeted cancer therapy". *Signal Transduct Target Ther* 2022;7:93.
45. Kalinovsky DV, Kibardin AV, Kholodenko IV, et al. Therapeutic efficacy of antibody-drug conjugates targeting Gd2-positive tumors. *J Immunother Cancer* 2022;10:e004646.
46. Raman S, Buongervino SN, Lane MV, et al. A Gpc2 antibody-drug conjugate is efficacious against neuroblastoma and small-cell

lung cancer via binding a conformational EPITOPE. *Cell Rep Med* 2021;2:100344.

47 Sano R, Krytska K, Larmour CE, *et al*. An antibody-drug conjugate directed to the ALK receptor demonstrates efficacy in Preclinical models of neuroblastoma. *Sci Transl Med* 2019;11:eaau9732.

48 Kendsersky NM, Lindsay J, Kolb EA, *et al*. The B7-H3-targeting antibody-drug conjugate M276-SL-PBD is potently effective against pediatric cancer Preclinical solid tumor models. *Clin Cancer Res* 2021;27:2938–46.

49 Dondero A, Morini M, Cangelosi D, *et al*. Multiparametric flow Cytometry highlights B7-H3 as a novel diagnostic/therapeutic target in Gd2Neg/low neuroblastoma variants. *J Immunother Cancer* 2021;9:e002293.

50 Ravi M, Paramesh V, Kaviya SR, *et al*. 3d cell culture systems: advantages and applications. *J Cell Physiol* 2015;230:16–26.

51 Bowers HJ, Fannin EE, Thomas A, *et al*. Characterization of Multicellular breast tumor Spheroids using image data-driven biophysical mathematical modeling. *Sci Rep* 2020;10:11583.

52 Rubie H, Chisholm J, Defachelles AS, *et al*. Phase II study of Temozolomide in Relapsed or refractory high-risk neuroblastoma: a

joint Société Française des cancers de L'Enfant and United Kingdom children cancer study group-new agents group study. *J Clin Oncol* 2006;24:5259–64.

53 Mody R, Naranjo A, Van Ryn C, *et al*. Irinotecan-Temozolomide with Temsirolimus or Dinutuximab in children with refractory or Relapsed neuroblastoma (COG Anbl1221): an open-label, randomised, phase 2 trial. *Lancet Oncol* 2017;18:946–57.

54 Di Giannatale A, Dias-Gastellier N, Devos A, *et al*. Phase II study of Temozolomide in combination with Topotecan (TOTEM) in Relapsed or refractory neuroblastoma: a European innovative therapies for children with cancer-SIOP-European neuroblastoma study. *European Journal of Cancer* 2014;50:170–7.

55 Le Teuff G, Castaneda-Heredia A, Dufour C, *et al*. Phase II study of Temozolomide and Topotecan (TOTEM) in children with Relapsed or refractory Extracranial and central nervous system tumors including Medulloblastoma with post hoc Bayesian analysis: A European ITCC study. *Pediatric Blood & Cancer* 2020;67. 10.1002/pbc.28032 Available: https://onlinelibrary.wiley.com/toc/15455017/67/1